^{69,71}Ga NMR spectra and relaxation in wurtzite GaN

M. Corti and A. Gabetta
Department of Physics "A. Volta" and Unita' INFM di Pavia, I-27100 Pavia, Italy

M. Fanciulli
Laboratorio MDM-INFM, Via C. Olivetti 2, 20041 Agrate Brianza, Italy

A. Svane and N. E. Christensen
Institute of Physics and Astronomy, University of Aarhus, DK-8000 Aarhus, Denmark

(Received 4 July 2002; published 26 February 2003)

Magnetic properties of wurtzite GaN are studied by Ga nuclear magnetic resonance (NMR) in a GaN bulk crystal containing a high carrier concentration, as well as in highly resistive Mg-doped crystals. The quadrupole coupling constant is derived from satellite lines and from the shift of the central line in the quadrupolar perturbed ^{69,71}Ga NMR spectra. The electric-field gradient is in good agreement with the value calculated by the *ab initio* full-potential linear-muffin-tin-orbital method, using the local-density approximation to describe exchange and correlation effects. The ^{69,71}Ga spin-lattice relaxations in the Mg-compensated sample in the range 80–400 K are due to the quadrupolar interaction mechanism, similar to what is observed in GaAs, and the proper scaling factor, given by the square of the ratio of the nuclear quadrupole moments, $(^{69}Q/^{71}Q)^2$, is observed for the two isotopes. In contrast, in the conductive sample, the relaxation mechanism is caused by magnetic interaction with the conduction electrons and one finds a relaxation rate, $W \propto T$. The isotope ratio $^{69}W/^{71}W$ is close to $(^{69}\gamma/^{71}\gamma)^2$, where γ is the gyromagnetic factor. Only above 200 K, there is evidence of a relaxation process due to interactions with phonons also in the degenerate sample, with a temperature dependence approximately of the form $W \propto T^3$, consistent with a Debye temperature around 600 K.

DOI: 10.1103/PhysRevB.67.064416 PACS number(s): 76.60.−k, 71.15.Mb

I. INTRODUCTION

GaN is a wide band-gap semiconductor which crystallizes in the hexagonal wurtzite structure. It is extensively considered for many optoelectronics and microelectronics devices such as blue-light-emitting diodes, ultraviolet lasers, and high-temperature, high-field heterojunction bipolar devices.[1] Recently, the spintronic application potential of this semiconductor has been tested by measuring the electron-spin coherence and dephasing in *n*-type GaN epilayers using time-resolved Faraday rotation.[2]

Bulk GaN single crystals can be grown in the wurtzite crystal structure using high-pressure and high-temperature methods.[3,4] Small needles or platelets having a very high crystal quality and a very high concentration of free electrons have been obtained. Semiinsulating transparent platelets can also be grown by doping the crystals with Mg.[5] The *n*-type conductivity of the as-grown samples is due to native defects. The nature of these residual donors is still controversial and either the N vacancy[6] or the Ga antisite[7] have been proposed. Mg-doped GaN samples are highly resistive and transparent. The dimensions of these crystals are suitable for conventional nuclear magnetic resonance (NMR) and relaxation measurements, which due to sensitivity problems, are impossible on epilayers. In addition, the availability of both conductive and resistive samples allows the investigation of the influence of the carriers on the NMR spectra and relaxation mechanisms.

The electric-field gradient (EFG) tensor $\bar{\bar{V}}$ is related to the nonspherical part (in fact, the $\ell=2$ component) of the crystalline Hartree potential $V_{H,\ell=2}$. The tensor elements are

$$V_{ij}=\frac{\partial^2 V_{H,\ell=2}}{\partial x_i \partial x_j}. \tag{1}$$

Denoting the eigenvalues of $\bar{\bar{V}}$ by V_{xx}, V_{yy}, and V_{zz} with $|V_{xx}| \leqslant |V_{yy}| \leqslant |V_{zz}|$, the EFG per definition is equal to V_{zz}, while the asymmetry parameter

$$\eta=\frac{V_{xx}-V_{yy}}{V_{zz}} \tag{2}$$

lies in the range $[0,1]$ (since $V_{xx}+V_{yy}+V_{zz}=0$). Due to the symmetry of the wurtzite crystal structure, the major axis of the EFG tensor ("z direction") is along the c axis, and η is zero.

The EFG at the regular Ga lattice position was earlier determined to be 6.75×10^{20} V/m^2 using magic angle sample-spinning nuclear magnetic resonance measurements (MASS NMR) on GaN powder.[8] However, data have been analyzed using a nonzero η parameter equal to 0.25 which is not consistent with the hexagonal wurtzite crystal structure. Optically detected electron nuclear magnetic resonance (ODENDOR) gave[9] $V_{zz}=6.5\pm0.2\times10^{20}$ V/m^2 at a defective Ga site assumed to be interstitial. Overhauser shift double-resonance experiments on the donor[10,11] yielded the EFG value $7.053\pm0.04\times10^{20}$ V/m^2. The double-resonance data were consistent with an axially symmetric EFG tensor, i.e., $\eta=0$. The ODENDOR as well as the Overhauser shift experiments detect mainly nuclei of the defect or nearby the defect, while NMR detects all nuclei in the crystal. However,

0163-1829/2003/67(6)/064416(8)/$20.00 ©2003 The American Physical Society

due the delocalized nature of the defect wave function, the hyperfine coupling is with many nuclei and the measured EFG should be very close to the EFG determined by NMR.[11]

In this paper, we report NMR measurements of the EFG in bulk GaN having the wurtzite structure. Both highly conductive *n*-type crystals and Mg-doped resistive crystals have been analyzed. The experimental data are compared with calculations based on the *ab initio* full-potential linear-muffin-tin-orbital (LMTO) method, where the local-density approximation (LDA) to the density-functional theory has been used to describe exchange and correlation effects. The Ga nuclear-spin dynamics in GaN has also been investigated in the temperature range 10–400 K. The influence of the free carriers on the EFG and on the relaxation mechanisms is discussed.

II. EXPERIMENTAL DETAILS

GaN bulk crystals in the wurtzite structure were grown from a gallium solution with a high-pressure method.[3,4] Crystals grow in the form of platelets 4–10 mm in diameter and having a 0.1 mm thickness. The GaN crystals are highly conductive, showing metallic behavior, in the temperature range 4.2–300 K, with free-electron concentration of 10^{19}–10^{20} cm^{-3} and mobilities in the range of 30–90 cm^2/Vs, independent of temperature.[12]

The NMR measurements were carried out on single crystals having different free-electron concentrations: Sample I, with an electron concentration of about 5×10^{19} cm^{-3} as derived from the longitudinal-optical phonon-plasmon coupled-mode frequency,[12,13] and sample II, a highly resistive Mg-doped GaN crystal.

The NMR measurements have been performed by means of a BRUKER MSL 200 Fourier-transform (FT) spectrometer and a MID-CONTINENT spectrometer, mainly at the magnetic-flux densities 9 and 1.5 T, corresponding to the resonance frequencies $^{69}\nu_L \cong 92$ MHz, $^{71}\nu_L \cong 116$ MHz and $^{69}\nu_L \cong 16.5$ MHz, $^{71}\nu_L \cong 20.4$ MHz, respectively. The line shape for the central $(+1/2 \leftrightarrow -1/2)$ transition was obtained by Fourier transforming the free-induction decay or collecting and then FT the second half of the echo signal. The complete spectra including the satellite lines were measured from the envelope of the echo intensity as a function of the irradiating frequency. The extra broadening of the line induced by the radio-frequency (rf) spectral distribution (~ 100 kHz) does not affect the determination of the satellite line positions. The ^{69,71}Ga nuclear-spin-lattice relaxation was studied by monitoring the echo intensity $m(t)$ as a function of the time t after a saturation sequence $[m(0)=0]$. The relaxation rate W was extracted from the behavior of the normalized recovery function

$$y(t)=[m(\infty)-m(t)]/m(\infty), \tag{3}$$

taking into account the solutions of the master equations for the populations of the Zeeman levels with the proper initial conditions induced by the saturating rf pulses (see Sec. III C).

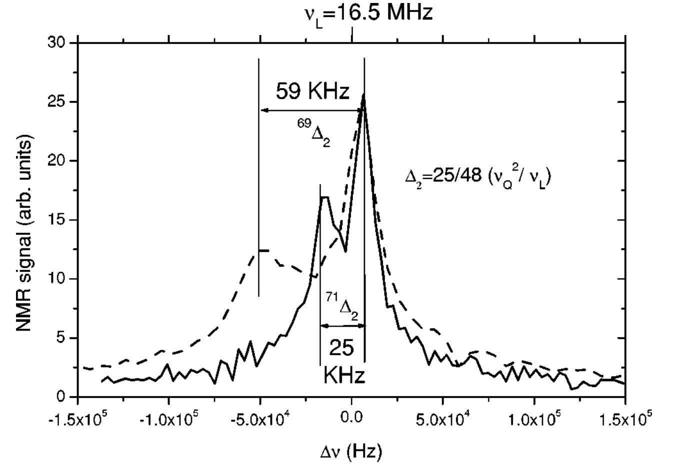

FIG. 1. Central line NMR spectra at 16.5 MHz for ^{71}Ga (solid line) and for ^{69}Ga (dashed line), as obtained from Fourier transform of the half echo signal in powdered GaN.

III. RESULTS AND DISCUSSION

A. Spectra and estimates of EFG

Due to the presence of the EFG related to the noncubic symmetry, ^{69,71}Ga ($I=3/2$ for both isotopes) NMR lines are split into three components. The central line transition $(+1/2 \leftrightarrow -1/2)$ is affected by the quadrupole interaction to the second order, while the satellite lines $(\pm 3/2 \leftrightarrow \pm 1/2)$ are shifted to the first order by an amount depending on the angle between the z axis (along c) and the external magnetic field. The quadrupolar coupling constant is related to V_{zz} through $\nu_Q = eQV_{zz}/2h$, where Q is the nuclear quadrupole moment and h is Planck's constant. A first, rough estimate of ν_Q was obtained for a powderlike sample consisting of many small single crystals. In the powder sample, the pulse length maximizing the ^{69,71}Ga NMR signals is close to half of the $\pi/2$ pulse for Ga nuclei in a reference solution, supporting the conclusion that the satellite lines are practically not irradiated.[14] For the central line, in the case of axial symmetry as in the hexagonal GaN, an asymmetric shape is expected, with two peaks separated by[14] $\Delta_2 = 25/48\nu_Q^2/\nu_L$. In Fig. 1, the FT of half of the echo signal for the two Ga isotopes at 16.5 MHz are reported. A good echo signal-to-noise ratio was obtained with a $(\pi/2)-\pi$ rf pulse separation of 100 μs. In fact, the dephasing time of the echo signal turns out $^{71}T_2 = 700$ μs and $^{69}T_2 = 550$ μs. These values indicate that the source of the intrinsic spin-spin relaxation is the dipole-dipole interaction since the local field at the Ga site is of the order of 0.4 Oe. If an intrinsic Gaussian dipolar broadening of the lines is assumed, the separation between the peaks leads to $^{71}\Delta_2 = 25$ kHz and $^{69}\Delta_2 = 59$ kHz, corresponding to a $^{71}\nu_Q = 0.89$ MHz and $^{69}\nu_Q = 1.37$ MHz, respectively. For ^{71}Ga, ν_Q was also measured from the separation between the satellite lines symmetrically, placed with respect to the central line and caused by the first-order quadrupolar effects, giving $^{71}\nu_Q = 0.85$ MHz. In order to achieve a better estimate of the EFG and to evidence a possible contribution due to the conduction electrons, the measurements have also been performed in small single crystals

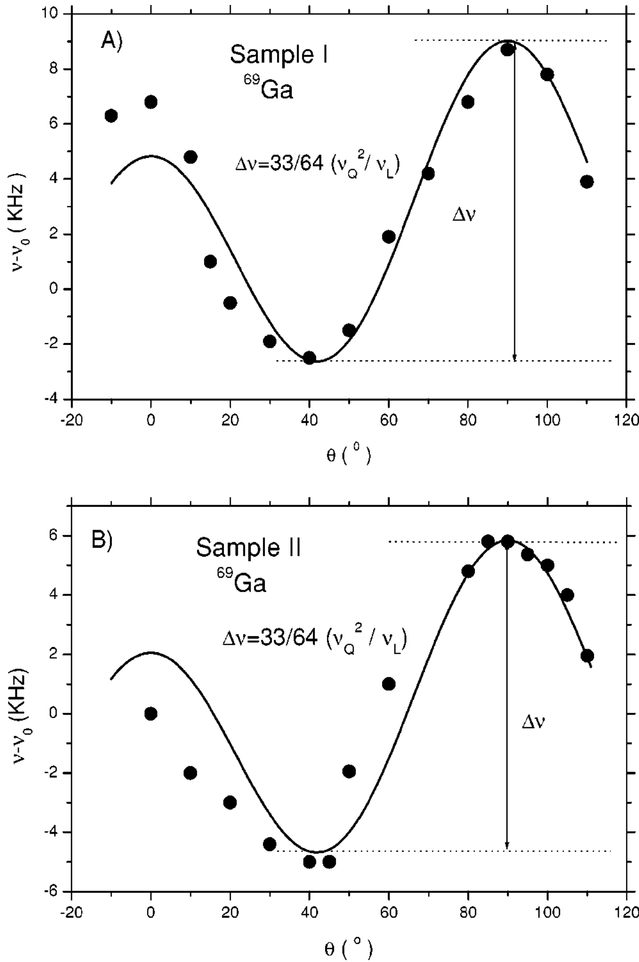

FIG. 2. ^{69}Ga rotation pattern for highly conductive GaN (sample I) (a); and for Mg-doped GaN (sample II) (b). The solid curves show best fits according to the theoretical expression for the second order quadrupolar shift of the central line.

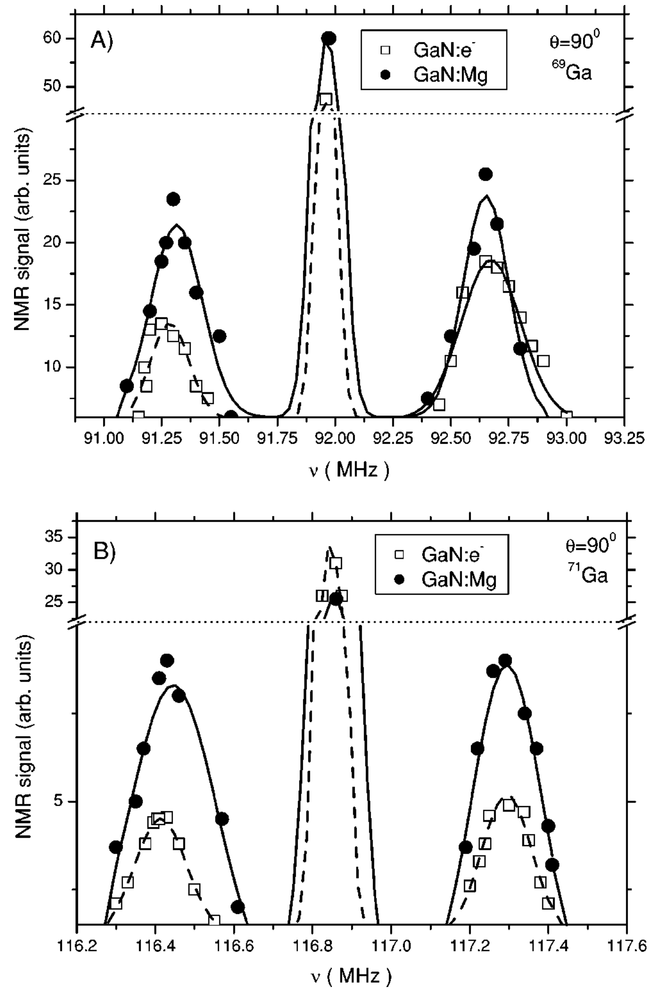

FIG. 3. Echo envelope spectra for ^{69}Ga (a); and for ^{71}Ga isotope (b), in highly conductive and in Mg-doped GaN crystals. The spectra were taken with the crystal c axis (z direction) perpendicular to the magnetic field, where the satellite separation is $2\nu_Q$.

with and without carrier-compensating Mg impurities. In single crystals, both the second-order shift of the central line and the first-order shift of the satellite lines as a function of the angle θ between the magnetic field **B** and the z direction were measured for ^{69}Ga and ^{71}Ga at $B=9$ T. From the total amplitude of the central line shift as a function of the angle θ, [see Figs. 2(a,b)], namely, $\Delta\nu=S_{\theta=\pi/2}-S_{\theta=\pi/4}$ and from the expected expression[14] $\Delta\nu=33/64\nu_Q^2/\nu_L$, one derives $^{69}\nu_Q=1.41$ MHz for sample I and $^{69}\nu_Q=1.43$ MHz for sample II. From the first-order shift of the satellite lines (Figs. 3), one obtains $^{69}\nu_Q=1.38$ MHz and $^{71}\nu_Q=0.88$ MHz for sample I and $^{69}\nu_Q=1.35$ MHz and $^{71}\nu_Q=0.86$ MHz for sample II. The values of ν_Q are practically identical, within the experimental error of ± 30 kHz, in the doped and undoped samples, indicating that the EFG is not significantly affected by the conduction electrons. The quadrupolar coupling constants $^{69}\nu_Q=1.38$ MHz and $^{71}\nu_Q=0.88$ MHz correspond to the EFG values $^{69}V_{zz}=6.77\times10^{20}$ V/m^2 and $^{71}V_{zz}=6.88\times10^{20}$ V/m^2, respectively. Since the two isotopes are in equivalent positions, the almost equal EFG values indicate that the electric-field gradient is primarily caused by the charges surrounding the nuclei, while polarizations induced by the nuclear quadrupole moment itself are of minor importance.[15] A summary of the data is given in Table I.

The rotation patterns for ^{69}Ga in GaN single crystals (sample I and sample II) shown in Fig. 2 are shifted relative

TABLE I. Quadrupolar coupling constants and EFG data. Present work, from the shift of the central line (a), from the satellites (b); MASS-NMR on powders (Ref. 8) (c); ODMR on epilayers (Ref. 9) (d); Overhauser shift double resonance (Ref. 9) (e). The coupling constants ν_Q are in MHz, and the EFGs, V_{zz}, in units of 10^{20} V/m^2.

	Sample I		Sample II	
	^{69}Ga	^{71}Ga	^{69}Ga	^{71}Ga
ν_Q (a)	1.41		1.43	
ν_Q (b)	1.38	0.88	1.35	0.86
V_{zz}	6.77	6.88	6.65	6.72
ν_Q (c)	1.4	0.85		
ν_Q (d)	1.32	0.84		
ν_Q (e)	1.432	0.906		

to each other by ≈3 kHz. This is probably due to the hyperfine interaction with the conduction electrons. However, a quantitative analysis is difficult as the estimated experimental error is almost of the same magnitude.

B. Theoretical calculation of EFG

The hexagonal phase of GaN has the wurtzite structure, space group No. 186 ($P6_3mc$) with atoms in the Wyckoff $2b$ positions, Ga :(1/3,2/3,0) and N: ($1/3,2/3,u$). The experimental[16–18] values of the axial ratio $c/a=1.627$ and the c-axis bond-length parameter $u=0.377$ are rather close to the ideal values $\sqrt{8/3}$ and 3/8. These parameters were also found in Mg-doped samples.[18]

The wurtzite-GaN calculations included in Ref. 19 were performed with ideal structural parameter values, it was demonstrated[20] in the case of AlN that even small changes in c/a and u produce significant changes in the band structure, in particular, at the valence-band top. Also, since the structural parameters vary with applied pressure,[20] it follows that deformation potentials involving gap edge states can only be accurately calculated if the volume dependence of c/a and u is properly taken into account.

Using all-electron *ab initio* total-energy minimization as in the case[20] of AlN, we have now determined theoretical structural parameters for GaN, and we further demonstrate that the electrical-field gradients are very sensitive to the values of these internal parameters. Denninger and Reiser[10] measured the EFG's on Ga as well as on N in GaN, and it is shown below that a set of ($c/a,u$) can be determined such that the calculated EFG values agree simultaneously with the experimental data for both atoms, and that these structural parameters are close to what was obtained by x-ray diffraction[16] and by total-energy optimizations.

The electronic structure of GaN was calculated within the LDA to the density-functional theory, and the one-electron Schrödinger-like equation was solved by means of the LMTO band-structure method[21] in a full-potential (FP) implementation.[22,23] This method expands the electron wave functions in terms of muffin-tin orbitals,[21] which are atom-centered Neumann functions augmented inside muffin-tin spheres by the numerical solution of the radial scalar-relativistic Dirac equation in the self-consistent crystal potential, together with the energy derivative of this solution. This construction has proven very accurate for solid-state calculations.[24] We used three different decay constants for the envelope functions. The basis set used included for Ga as well as N in the valence-band regime 3 orbitals of s character, 3×3 orbitals of p character, 3×5 orbitals of d character, and 2×7 orbitals of f character (in short: $3s$, $3p$, $3d$, $2f$). The semicore Ga-$3d$ states were included among the valence states in the form of "local orbitals."[25] Polarization effects on lower-lying core states are assumed to be insignificant for the EFG values.[15] No shape approximation for the crystal potential is invoked. The crystalline charge density is evaluated exactly within muffin-tin spheres, while in the interstitial region, an interpolation scheme is used to obtain the charge density.[22] To further increase the accuracy of the interpolation scheme, additional "empty" muffin-tin spheres

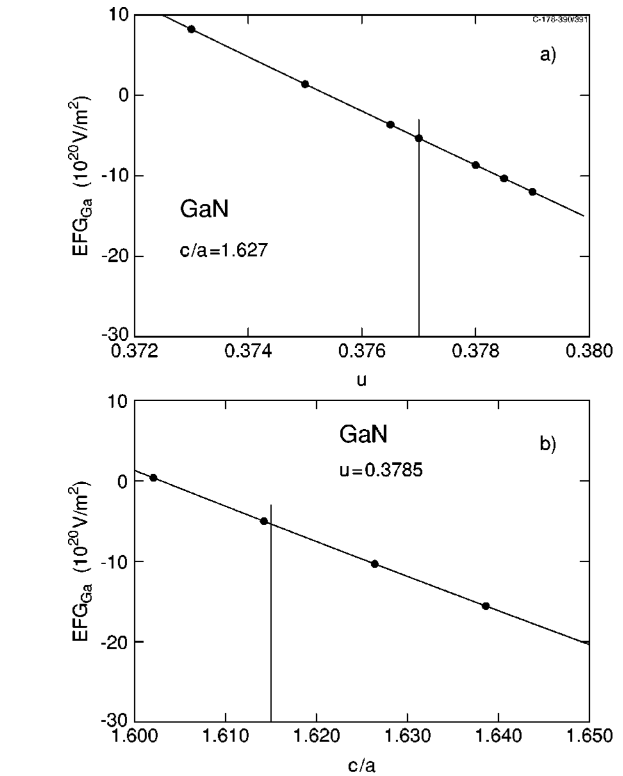

FIG. 4. Calculated electrical-field gradients, EFG_{Ga} on the Ga site in GaN. In the upper figure (a), the c/a ratio was kept fixed a 1.627, the experimental value. The vertical line marks the experimental value of u. In (b) u is fixed to 0.3785, the value obtained in the present total-energy optimizations. Here the vertical line marks the c/a value calculated by the total-energy optimizations.

are included in the open regions of the unit cell. Although usually not needed, we included a few orbitals (s like) on the empty-site positions in the basis set since these affected the EFG values by ≈1%.

At ambient conditions, the experimental[16] lattice constants of GaN are $a=3.190$ Å and $c=5.189$ Å. Keeping the volume fixed, and equal to its experimental value, we found that the structural parameters which minimize the LDA total energy are $c/a=1.616$ and $u=0.3785$. Other *ab initio* calculations also gave results close to the experimental[16] values. Using a plane-wave basis and pseudopotentials, Yeh *et al.*[26] found ($c/a,u$)=(1.633,0.378) without inclusion of the Ga-$3d$ states as valence states. Wright and Nelson[27] used a similar method, but included the $3d$ states, and found (1.626,0.3770), i.e., almost the same values as measured.[16] Kim *et al.*[28] determined the parameters to be (1.62,0.379). If our values are rounded off, they coincide with these, and this is not unexpected since Kim *et al.* also used FP-LMTO and LDA, and the codes are very similar.[22] Fixing c/a to its experimental value, Wei and Zunger[29] found $u=0.3768$.

The calculated values of the EFG's depend sensitively on the structural parameters. For example, assuming an error bar of ±1 per mil on u, we obtain $EFG_{Ga}=-5.1\pm1.3\times10^{20}$ V/m^2 for the experimental[16] ($c/a,u$). For the Ga site in GaN, this is illustrated in Fig. 4, where (a) shows the variation with u for fixed c/a (the experimental value) and

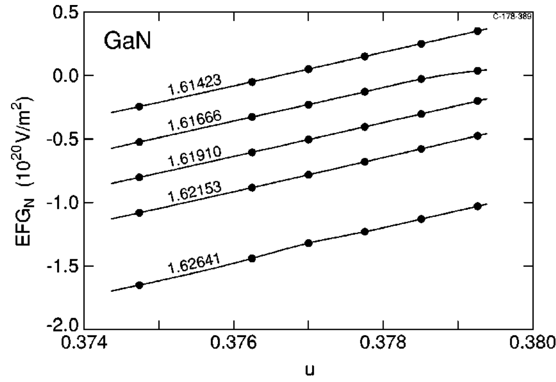

FIG. 5. Calculated electrical-field gradients, EFG_N on the N site in GaN vs u for selected c/a values.

(b) gives the variation of EFG_{Ga} with c/a when u is kept at the theoretical value (0.3785) obtained by the present optimization. The vertical lines in (a) and (b) mark the *experimental* u value, and the *theoretical* c/a value, respectively. The corresponding calculated EFG_{Ga} values are almost identical, -5.33×10^{20} V/m^2. In magnitude, this is a little smaller than found in the present experiment and thus also smaller than the values 7.053×10^{20} V/m^2 and 7.046×10^{20} V/m^2, $\pm0.004\times10^{20}$ V/m^2, measured by Denninger and Reiser[10] for ^{69}Ga and ^{71}Ga, respectively. The calculation represented in Fig. 4 alone does not allow us to select the "best" set of structural parameters. However, this can be done if the EFG on N is taken into account. Figure 5 shows how EFG_N varies with u for a set of fixed c/a values. The experimental[10] value of the magnitude of EFG_N is $0.788\pm0.02\times10^{20}$ V/m^2. From the full set of calculated field gradients vs c/a and u, we determined the relations between the parameters which fulfill $EFG_{Ga}(c/a,u)=-7.053$ and $EFG_N(c/a,u)=-0.788$, in units of 10^{20} V/m^2. The results are shown in Fig. 6 as two nearly straight lines. These cross at $(c/a,u)=(1.6230,0.3780)$, and this is then the parameter set, for which the calculated EFG's for Ga as well as N agree with the experiments of Ref. 10. The theoretical calculations mentioned above, and the x-ray results, are also marked in Fig. 6.

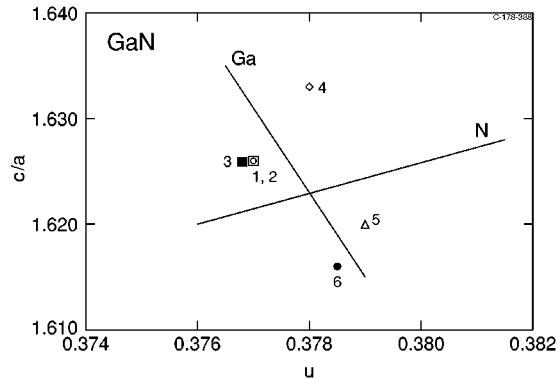

FIG. 6. The lines define the structural parameters for which EFG_{Ga} and EFG_N are equal to the experimental results of Ref. 10. Theoretical and experimental c/a and u values are shown as symbols: 1, Ref. 16 (x-ray diffraction); 2, Ref. 29 (full potential linear augmented plane waves, with c/a fixed); 3, Ref. 27 (pseudopotentials, Ga 3d as valence); 4, Ref. 26 (pseudopotentials, Ga 3d in core); 5, Ref. 28 (full potential LMTO); 6, Present (full-potential LMTO).

Some of the samples used in the experiments have excess electron concentration. Since this might affect the values of the EFG's, we performed calculations for different doping levels. This was simply done by defining a suitable Fermi level in the conduction-band regime, and subsequently, deriving the electron concentration and EFG values. The structural parameters were kept fixed, chosen to be $c/a=1.6264$, $u=0.377$. The results obtained are for four electron concentrations (in units of 10^{20} cm^{-3}) (0.0,2.2,4.4,22.0): $EFG_{Ga}=(-5.054,-5.059,-5.063,-5.134)\times10^{20}$ V/m^2 and $EFG_N=(-1.055,-1.062,-1.066,-1.114)\times10^{20}$ V/m^2.

This shows that variation in the electron concentration only weakly affects the field gradients, in agreement with the experimental data.

C. ^{69,71}Ga relaxation mechanisms

The NMR relaxation mechanism was studied through the temperature behavior of the relaxation rates (in the range from 10 to 400 K) and by comparing the relaxation rates of the two isotopes. Furthermore, the recovery laws also can provide some insights into the relaxation mechanisms. For a relaxation process driven by the time-dependent quadrupole interactions, the recovery function, Eq. (3), for $I=3/2$ is given by the expression

$$y(t)=\tfrac{1}{2}\exp(-2W_{Q1}t)+\tfrac{1}{2}\exp(-2W_{Q2}t), \quad (4)$$

where W_{Q1} and W_{Q2} are the transition rates for $\Delta m=1$ and $\Delta m=2$, respectively. In the powdered sample, one can assume $W_{Q1}\cong W_{Q2}\equiv W_Q$ and an exponential recovery is practically observed.[30] For a magnetic relaxation mechanism, associated with the fluctuations of the local magnetic field at the positions of the ^{69,71}Ga nuclei, and in the presence of static quadrupole interaction, the recovery function is given by

$$y(t)=c\exp(-12W_mt)+(1-c)\exp(-2W_mt), \quad (5)$$

where W_m is the magnetic transition probability. The constant is $c=0.6$ for irradiation of the central line with a rf pulse sequence much longer than the corresponding transition rate W_m^{-1} (long irradiation) and $c=0.9$ for irradiation of the central line with a single rf pulse (short irradiation).[31] The measurements have been performed in magnetic fields of 9 and 1.6 T. In sample I, a recovery law given by two exponentials is evidenced, with $c=0.65$, typical of a relaxation process driven by magnetic interactions with the initial condition intermediate between the short irradiation and the long irradiation. The behavior of the ^{69,71}Ga relaxation rates as a function of temperature is shown in Fig. 7. Between 10 and 150 K, the relaxation rates display linear T dependence and the isotope ratio is close to the value expected for a magnetic relaxation mechanism,[14] $^{69}W/^{71}W=(^{69}\gamma/^{71}\gamma)^2\approx2/3$, where γ is the gyromagnetic factor. Above 150 K, the relaxation rate is no longer linear in T and the ratio $^{69}W/^{71}W$

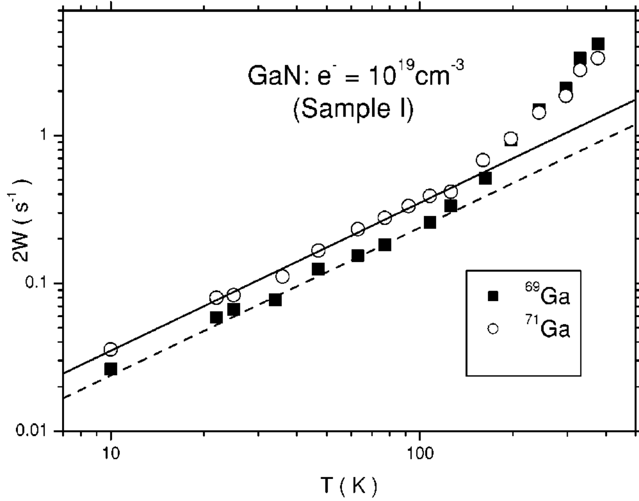

FIG. 7. ^{69}Ga (filled squares) and ^{71}Ga (open circles) relaxation rates for the highly conductive GaN crystal (sample I) as a function of temperature. The solid line indicates a linear T dependence expected for a magnetic relaxation mechanism. The dashed line corresponds to the same relaxation mechanism scaled by the squared gyromagnetic ratio $(^{69}\gamma/^{71}\gamma)^2 \approx 2/3$.

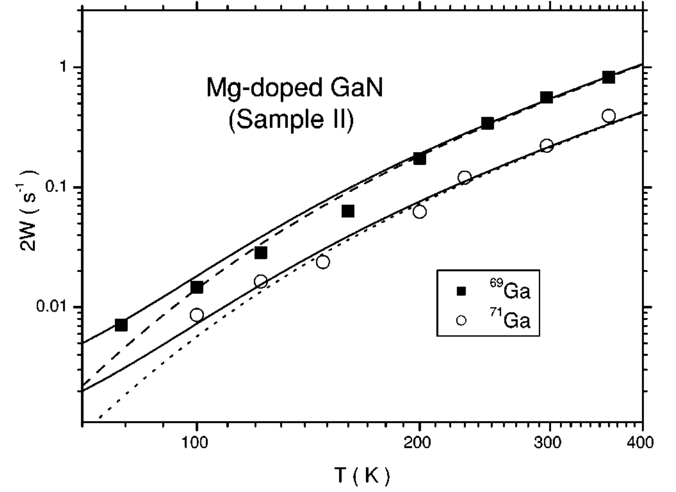

FIG. 8. ^{69}Ga (full squares) and ^{71}Ga (open circles) relaxation rates as a function of the temperature in the Mg-doped GaN crystal and comparison with the theoretical relaxation rates for the two-phonon Raman relaxation mechanism, Eq. (6) for ^{69}Ga (dashed line) and for ^{71}Ga (dotted line). The solid lines indicate the behaviors obtained by adding, at low temperature, a contribution to the relaxation rate of magnetic origin (see text).

increases. In the temperature range 150–250 K, the relaxation rates for the two isotopes are nearly equal, while above 300 K, ^{69}W is larger than ^{71}W, and the temperature dependence is approximately of the form $W \propto T^3$. In that temperature range, the recovery function is well approximated by a single exponential. These characteristics suggest that at high temperatures, the relaxation rates contain a significant contribution from two-phonon Raman scattering. For this relaxation mechanism, the relaxation rate may be calculated in the Debye model as[14]

$$W(T) \propto Q^2 \left(\frac{T}{\theta_D}\right)^7 \int_0^{\theta_D/T} \frac{x^6 e^x dx}{(e^x-1)^2}, \tag{6}$$

where Q is the quadrupole moment, $x = h\omega/2\pi K_B T$, and θ_D the Debye temperature. This expression behaves as $W \propto T^7$ for $T \ll \theta_D$, crossing over to a $W \propto T^2$ behavior for $T \gg \theta_D$. The departure of the relaxation rate in Fig. 7 at high T from the T^2 law indicates that the condition $T \gg \theta_D$ is not valid. This is consistent with the reported Debye temperature for GaN $\theta_D \approx 600$ K.[32,33]

The Ga relaxation rate as a function of temperature for the Mg-doped GaN crystal are reported in Fig. 8. The fact that the recovery of the nuclear magnetization is single exponential, together with the finding that the ratio $^{69}W/^{71}W \simeq 2.5$ supports the conclusion of a quadrupolar two phonon Raman relaxation mechanism, similar to what is found in GaAs.[34] For $T \geqslant 150$ K, in fact, the behaviors for the two isotopes are well reproduced by the two-phonon Raman expression, Eq. (6), with $\theta_D \simeq 600$ K (see the dashed and dotted lines in Fig. 8). Below ~ 150 K, the ratio of the relaxation rates for the two isotopes start changing with respect to the value given by $(^{69}Q/^{71}Q)^2$. If one adds at low temperature a contribution to the relaxation rate of magnetic origin, around $4 \times 10^{-5} T$, one can account for the deviation from the expected quadrupole relaxation mechanism. A numerical computation of the relaxation rates taking into account both magnetic and quadrupolar contributions would therefore reproduce the experimental W temperature behavior over the whole temperature range (see Fig. 8 solid lines).

As regards the conduction-electrons contribution to the relaxation, this is proportional to the square of the electron density at the nucleus (the contact density), while the Knight shift K is proportional to the contact density. Hence, a simple relation between the relaxation rate W and K may be expressed as the Korringa ratio[14]

$$R = \frac{K^2}{W}\frac{T}{S} = 1, \tag{7}$$

where $S = (\gamma_e/\gamma_n)^2 h/(8\pi^2 k_B)$. Equation (7) holds for metals, and it is only valid for (free) carriers in a semiconductor if the donor levels (considering n type) are resonant with the conduction band. The fact that the relaxation rate for the conducting sample is found to be proportional to T indicates that this is the case here, in agreement with the measured carrier concentration. Taking the Knight shift of Ga in GaN from Fig. 2, i.e., $K \simeq 3$ KHz, and the low-T limiting behavior of W/T from Fig. 7, we compute $R = 0.1$. The significant deviation from the value $R = 1$ is likely to be due to a relaxation contribution from non-s electrons, which increases the relaxation rate, but leaves K unaffected.

IV. CONCLUSIONS

In this paper, we have reported and discussed the results of a comprehensive NMR study of various samples of GaN, performed by carrying out measurements of spectra and re-

laxation rates, for both the ^{69}Ga and ^{71}Ga isotopes and at different magnetic fields. From the second-order shift of the central line and from the first-order shift of the satellite lines, the quadrupolar coupling constant has been derived and compared with theoretical *ab initio* calculations performed within the local-density approximation to density-functional theory, and implemented with the full-potential-LMTO method.

The good agreement between the calculated Ga EFG and the one derived from the observed satellite line shifts supports the analysis of the present experiments. Further, the calculations illustrate that the EFG's are very sensitive to variations in structural parameters.

Furthermore, it has been shown that the contribution to the electric-field gradients from the conduction electrons is negligible, as indicated by the almost equal quadrupole coupling constants obtained in the sample without carriers and in the one with a carrier concentration of about 10^{19} cm^{-3}. The calculations also corroborate this finding.

The spin-lattice relaxation measurement has provided insights into the time-dependent interactions driving the recovery towards equilibrium and on their temperature dependence. In sample I, with relatively high carrier concentration, the relaxation process is up to about 200 K dominated by the conduction-electron scattering from the nuclei. The relaxation rates W follow the linear-temperature dependence and the rates for the two isotopes scale according to the square of the ratio of the gyromagnetic factors. The Korringa factor $R = K^2T/WS$ is about 0.1, suggesting a contribution to the relaxation from non-s electrons. Above about 200 K, the relaxation in the conductive sample progressively becomes dominated by two-phonon Raman processes. The temperature variation departs from a linear-T dependence, and the ratio of the relaxation rates for the two isotopes deviates more and more from the square of the ratio of the gyromagnetic factors approximating the ratio of the quadrupole moments $(^{69}Q/^{71}Q)^2$. In the highly resistive sample, the ratio of the relaxation rates for the two isotopes is close to $(^{69}Q/^{71}Q)^2$ and for $T \geqslant 150$ K, the W temperature behaviors are consistent with a two-phonon relaxation mechanism with a Debye temperature $\theta_D \simeq 600$ K. Only below ~ 150 K, the onset of a relatively small contribution to the relaxation of magnetic origin must be included.

ACKNOWLEDGMENTS

We are grateful to the High Pressure Research Center UNIPRESS, Warsaw, Poland for supplying the GaN samples. We would like also to thank Professor A. Rigamonti for his continuous interest and helpful discussions.

[1] H. Morkoc, Mat. Sci. Eng. Rep. **33**, 135 (2001).
[2] B. Beschoten, E. Johnston-Halperin, D.K. Young, M. Poggio, J.E. Grimaldi, S. Keller, S.P. DenBaars, U.K. Mishra, E.L. Hu, and D.D. Awschalom, Phys. Rev. B **63**, 121202 (2001).
[3] I. Grzegory and S. Krukowski, Phys. Scr., T **39**, 242 (1991).
[4] I. Grzegory, M. Bockowski, B. Lucznik, S. Krukowski, M. Wroblewski, and S. Porowski, MRS Internet J. Nitride Semicond. Res. **1**, 20 (1996).
[5] T. Suski, J. Jun, M. Leszczynski, H. Teisseyre, I. Grzegory, S. Porowski, G. Dollinger, K. Saarinen, T. Laine, J. Nissila, W. Burkhard, W. Kriegseis, and B.K. Meyer, Mater. Sci. Eng., B **B59**, 1 (1999).
[6] M. Ilegems and M.C. Montgomery, J. Phys. Chem. Solids **34**, 885 (1973).
[7] P. Boguslawski, E.L. Briggs, and J. Bernholc, Phys. Rev. B **51**, 17 255 (1995).
[8] O.H. Han, H.K. Timken, and E. Oldfield, J. Chem. Phys. **89**, 6046 (1988).
[9] F.K. Koschnick, K. Michael, J.-M. Spaeth, B. Beaumont, and P. Gibart, Phys. Rev. B **54**, R11 042 (1996).
[10] G. Denninger and D. Reiser, Phys. Rev. B **55**, 5073 (1997).
[11] D. Reiser, J. Blömker, G. Denninger, and J. Schneider, Solid State Commun. **102**, 359 (1997).
[12] P. Perlin, J. Camassel, W. Knap, T. Taliercio, J.C. Chervin, T. Suski, I. Grzegory, and S. Porowski, Appl. Phys. Lett. **67**, 2524 (1995).
[13] E. Bonera and M. Fanciulli (private communication).
[14] A. Abragam, *The Principles of Nuclear Magnetism* (Clarendon Press, Oxford, 1961).
[15] J. Ehmann and M. Fähnle, Phys. Rev. B **55**, 7478 (1997).
[16] H. Schulz and K.H. Thiemann, Solid State Commun. **23**, 815 (1977).
[17] M. Leszczynski, H. Teisseyre, T. Suski, I. Grzegory, M. Bockowski, J. Jun, S. Porowski, K. Pakula, J.M. Baranowski, C.T. Foxon, and T.S. Cheng, Appl. Phys. Lett. **69**, 73 (1996).
[18] *Properties, Processing and Applications of Gallium Nitride and Related Semiconductors*, edited by J. H. Edgar, S. Strite, I. Akasaki, H. Amano, and C. Wetzel, EMIS Datareviews Series Vol. N23. (INSPEC, London, 1999).
[19] N.E. Christensen and I. Gorczyca, Phys. Rev. B **50**, 4397 (1994).
[20] N.E. Christensen and I. Gorczyca, Phys. Rev. B **47**, 4307 (1993).
[21] O.K. Andersen, Phys. Rev. B **12**, 3060 (1975).
[22] M. Methfessel, Phys. Rev. B **38**, 1537 (1988); M. Methfessel, C.O. Rodriguez, and O.K. Andersen, *ibid.* **40**, 2009 (1989).
[23] M. van Schilfgaarde and M. Methfessel (private communication).
[24] O. K. Andersen, O. Jepsen, and O. Glötzel, in *Canonical Description of the Band Structures of Metals*, Proceedings of the International School of Physics "Enrico Fermi," Course LXXXIX, Varenna, 1985, edited by F. Bassani, F. Fumi, and M. P. Tosi (North-Holland, Amsterdam, 1985), p. 59.
[25] D. J. Singh, *Planewaves, Pseudopotentials and the LAPW Method* (Kluwer Academic, Boston, 1994).
[26] C.Y. Yeh, Z.W. Lu, S. Froyen, and A. Zunger, Phys. Rev. B **46**, 10 086 (1992).
[27] A.F. Wright and J.S. Nelson, Phys. Rev. B **50**, 2159 (1994).
[28] K. Kim, W.R.L. Lambrecht, and B. Segall, Phys. Rev. B **53**, 2159 (1994).
[29] S.-H. Wei and A. Zunger, Appl. Phys. Lett. **69**, 2719 (1998).

[30] A. Rigamonti, Adv. Phys. **33**, 115 (1984).

[31] T. Rega, J. Phys.: Condens. Matter **3**, 1871 (1991).

[32] I. Akasaki and H. Amano, in *Properties of Group III Nitrides*, edited by J. H. Edgar (INSPEC, London, 1994), p. 30.

[33] X.L. Chen, J.K. Liang, X.P. Xu, T. Xu, P.Z. Jiang, Y.D. Yu, and K.Q. Lu, Mod. Phys. Lett. B **13**, 285 (1999).

[34] T.H. Yeom, I.G. Kim, S.H. Choh, K.S. Hong, Y.J. Park, and S.-K. Min, Solid State Commun. **111**, 229 (1999).